

Design and verification of a broadband highly-efficient plasmonic circulator

Jianfei Han(韩建飞), Shu Zhen(甄姝), Weihua Wang(王伟华), Kui Han(韩奎), Haipeng Li(李海鹏), Lei Zhao(赵雷), and Xiaopeng Shen(沈晓鹏)

Citation: Chin. Phys. B, 2020, 30 (**3**): 034102. DOI: 10.1088/1674-1056/abca23
Journal homepage: http://cpb.iphy.ac.cn; http://iopscience.iop.org/cpb

What follows is a list of articles you may be interested in

Ultra-compact graphene plasmonic filter integrated in a waveguide

Baoxin Liao(廖宝鑫), Xiangdong Guo(郭相东), Hai Hu(胡海), Ning Liu(刘宁), Ke Chen(陈科), Xiaoxia Yang(杨晓霞), Qing Dai(戴庆)

Chin. Phys. B, 2018, 27 (**9**): 094101. DOI: 10.1088/1674-1056/27/9/094101

Tunable coupling of a hybrid plasmonic waveguide consisting of two identical dielectric cylinders and a silver film

Benli Wang(王本立), Han Liang(梁涵), Jiafang Li(李家方)

Chin. Phys. B, 2017, 26 (**11**): 114103. DOI: 10.1088/1674-1056/26/11/114103

An electrically tunable metasurface integrated with graphene for mid-infrared light modulation

Zongpeng Wang(王宗鹏), Ya Deng(邓娅), LianFeng Sun(孙连峰)

Chin. Phys. B, 2017, 26 (**11**): 114101. DOI: 10.1088/1674-1056/26/11/114101

Optimization of loss and gain multilayers for reducing the scattering of a perfect conducting cylinder

Zhen-Zhong Yu(余振中), Guo-Shu Zhao(赵国树), Gang Sun(孙罡), Hai-Fei Si(司海飞), Zhong Yang(杨忠)

Chin. Phys. B, 2016, 25 (**7**): 074101. DOI: 10.1088/1674-1056/25/7/074101

Spoof surface plasmon-based bandpass filter with extremely wide upper stopband

Xiaoyong Liu(刘小勇), Lei Zhu(祝雷), Yijun Feng(冯一军)

Chin. Phys. B, 2016, 25 (**3**): 034101. DOI: 10.1088/1674-1056/25/3/034101

Design and verification of a broadband highly-efficient plasmonic circulator*

Jianfei Han(韩建飞)[1], Shu Zhen(甄姝)[1], Weihua Wang(王伟华)[1], Kui Han(韩奎)[1], Haipeng Li(李海鹏)[1], Lei Zhao(赵雷)[2], and Xiaopeng Shen(沈晓鹏)[1,†]

[1] School of Materials Science and Physics, China University of Mining and Technology, Xuzhou 221116, China
[2] School of Information and Control Engineering, China University of Mining and Technology, Xuzhou 221116, China

(Received 18 September 2020; revised manuscript received 19 October 2020; accepted manuscript online 13 November 2020)

Circulators play a significant role in radar and microwave communication systems. This paper proposes a broadband and highly efficient plasmonic circulator, which consists of spoof surface plasmon polaritons (SSPPs) waveguides and ferrite disks to support non-reciprocal mode coupling. The simulated performance of symmetrically designed circulator shows that it has an insertion loss of roughly 0.5 dB while the isolation and return loss is more than 12 dB in the frequency range of 6.0 GHz–10.0 GHz (relative bandwidth of 50%). Equivalent circuit model has been proposed to explain the operating mechanism of the plasmonic circulator. The equivalent circuit model, numerical simulations, and experimental results are consistent with each other, which demonstrates the good performance of the proposed plasmonic circulator.

Keywords: plasmonic, circulator, spoof surface plasmon polaritons, ferrite

PACS: 41.20.Jb, 73.20.Mf, 84.40.Az, 85.70.Ge **DOI:** 10.1088/1674-1056/abca23

1. Introduction

Circulators are widely used in radar and radio communication systems, which are used to realize one-way transmission function.[1–4] They play an important role in avoiding mutual interference between the transmitted and received signals. They also play a critical role in protecting the signal source. There has been extensive theoretical and experimental research on microstrip line, strip line, and the waveguides-based Y-junction circulators, which rely on the anisotropic permeability of YIG ferrite.[5–11] With the rapid development of modern science and an increasing demand of communication systems, different schemes have been proposed to realize circulators. In 2016, Liu *et al.* introduced magneto–optical materials into dielectric waveguides and proposed a four port circulator by exploiting the anisotropic permittivity of magneto–optical materials under the bias of external magnetic fields.[12] In 2019, Dmitriev *et al.* proposed a circulator based on the anisotropic permittivity of graphene materials under the bias of external magnetic fields.[13] Most of the circulator designs achieve one-way transmission by applying an external magnetic field to the gyroelectric or gyromagnetic material to break the symmetry of the permittivity or permeability tensor.[14–19] Non-magnetic material is also used to design circulators without using a magnetic field bias to break reciprocity.[20,21] These designs open up a way to design non-reciprocal devices based on different mechanisms.

Spoof surface plasmon polaritons (SSPPs) have received widespread attention at microwave frequencies,[22] whose properties are very similar to those of SPPs in the near-infrared and optical regions.[23,24] For example, SSPPs find similarities with SPPs in terms of dispersion relations, local field enhancement, sub-wavelength confinement and other characteristics. Shen *et al.* proposed a planar ultra-thin SSPPs waveguide that enables SSPPs to be transmitted along a curved, folded surface for a long distance.[25,26] This kind of planar guided wave structure has a strong field confining ability to SSPPs, and achieves low loss and high efficiency transmission. These works have greatly promoted the rapid development of plasmonic devices in microwave frequency region.[27–33] Recently, Pan *et al.* proposed a circulator which uses comb-like transmission lines to guide the signals.[34] The design is compact with insertion loss at about 0.5 dB in the frequency range of 10.6 GHz–11.5 GHz. It is still quite challenging to design a broadband and highly-efficient SSPPs based circulator and the physical mechanism of the working of plasmonic circulator needs to be clarified.

In this paper, we propose a wideband, low-loss and highly efficient plasmonic circulator. Structured metal stripes have been used as internal conductor of the circulator to guide the propagation of SSPPs. A static bias magnetic field has been applied to the ferrite and one-way transmission of SSPPs has been realized by using its anisotropy. The overall structure is completely symmetrical and has the same transmission and isolation performance once evaluated from different ports. The characteristic of the proposed plasmonic circulator has been verified through numerical simulations as well as experiments. At the same time, equivalent circuit model has been applied to evaluate the transmission, reflection and isolation

*Project supported by the Six-Talent-Peaks Project in Jiangsu Province of China (Grant No. XYDXX-072) and the National Natural Science Foundation of China (Grant No. 61372048).

†Corresponding author. E-mail: xpshen@cumt.edu.cn

© 2021 Chinese Physical Society and IOP Publishing Ltd

characteristics of the plasmonic circulator.

2. Design and analysis

2.1. Plasmonic circulator design

The structure model of the plasmonic circulator is shown in Fig. 1(a). The entire circulator consists of three SSPPs waveguides, two ferrite disks, two foams, and two ground planes. The thickness of the SSPPs waveguides is 0.018 mm and the substrate is F4B with thickness 0.1 mm and permittivity $\varepsilon_r = 2.65$. Two ferrite disks have been placed above and below the center conductor (triangle region) with radius $R = 6.5$ mm, height $h = 2$ mm. Yttrium–iron–garnet (YIG)-based ferrite has been used having a saturation magnetization of $4\pi M_s = 1850$ Gs (1 Gs = 10^{-4} T), resonance line width of $\Delta H = 10$ Oe (1 Oe = 79.5775 A·m^{-1}), and relative permittivity of $\varepsilon_f = 15$. Two foam boards with hollow center have been used to fix the YIG ferrite disks and support the metal ground. The SSPPs waveguide structure and related dimensions are shown in Fig. 1(b). Three waveguides with 120° rotational symmetry have been connected to the central conductor junction. Both sides of the SSPPs waveguides have been designed to have a blade-like metal structure and the transmission path is equal from all the ports. The CPW with the GND plane has been used as the feed of three ports. The transition part is composed of a gradient comb-shaped waveguide and flared ground on both sides, which improves the coupling efficiency of SSPPs. A transition has been designed which ensure impedance matching while transitioning from CPW to SSPPs mode. The length and width of the flared ground have been designed as $L_1 = 26$ mm, $L_2 = 12$ mm, and $W = 5$ mm. The comb unit structure has the parameter of period $p = 5$ mm, groove width $a = 2$ mm, and groove depth $h = 4$ mm.

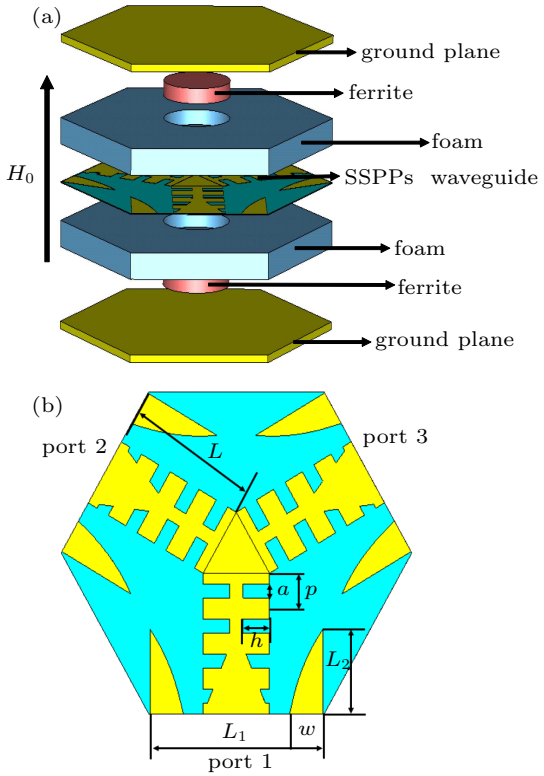


Fig. 1. Configuration of the proposed plasmonic circulator. (a) The structure model of the plasmonic circulator. (b) The structure diagram of the SSPPs waveguide and the corresponding structural parameters.

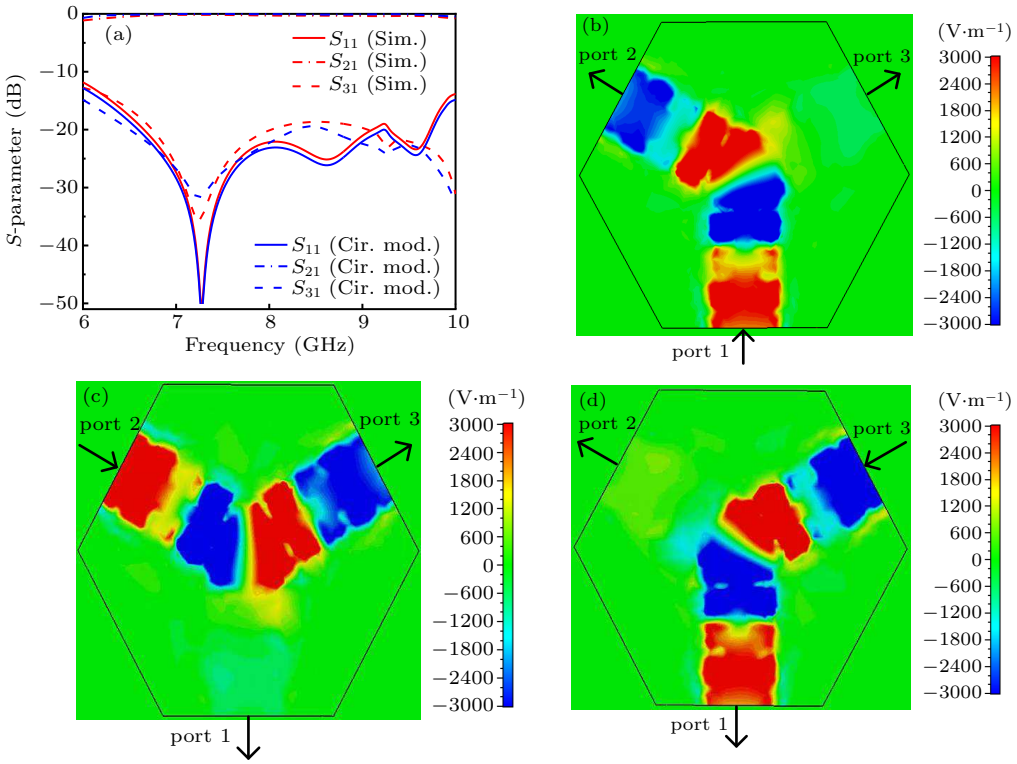


Fig. 2. (a) S-parameters of the simulation (Sim.) and the equivalent circuit (Cir.) model when electromagnetic wave incident from port 1. S_{11} (solid line) is the return loss, S_{21} (dash dot line) is the insertion loss, and S_{31} (dash line) is the isolation. (b)–(d) The E_z distribution of the electric field as incident from ports 1, 2, and 3 at frequency of 8 GHz, respectively.

We have analyzed the transmission characteristics of the circulator after applying a magnetic field of $H_0 = 1750$ Oe using CST Microwave Studio. Figure 2 shows the simulation results of circulator's insertion loss, isolation, and return loss and the distribution of the electric field in z direction when the wave is incident from port1. From the simulation results (red curves) in Fig. 2(a), it can be seen that the insertion loss is less than 0.5 dB in the frequency range of 6.0 GHz–10.0 GHz while the return loss and isolation are more than 12 dB. Due to the symmetric design of the circulator, no matter which port the signal is input from, we observed a consistent trend in all the S-parameter curves.

To visualize the performance of the circulator, we monitor the electric field at 8.0 GHz. Figure 2(b) shows the intensity distribution of the electric field (E_z) at $z = 0.5$ mm plane above SSPPs waveguide when the signal is input from port 1. Same magnitude of electric field intensity at port 1 and port 2, indicates that the resonance modes of the ferrite cavity can effectively transfer the signal to port 2. In contrast to that, energy transmitted from port 1 to port 3 is very small, which indicates that the resonance modes of the ferrite cavity are blocking the signal to port 3. Figures 2(c) and 2(d) show the intensity distribution of the electric field (E_z) at the $z = 0.5$ mm plane above the SSPPs waveguide when the signal is input from port 2 and port 3, respectively. The distribution of electric field in Fig. 2 proves that the input and output ports show a perfect cycle in a sequence of $1 \to 2$, $2 \to 3$, $3 \to 1$.

2.2. Equivalent circuit model analysis

In order to understand the working mechanism of the deigned plasmonic circulator, we have employed an equivalent circuit model. The model is represented by a series of LC circuits which helps analyze the performance of the circulator.[35,36] Equivalent circuit model has been widely used to analyze the working mechanism of absorber, filter, and circulator. Very recently it has also been used to analyze the transmission performance of SSPPs.[37–39] The LC circuit equivalent of plasmonic circulator is shown in Fig. 3. In this model, the capacitor C is formed between the central conductor junction and the grounding plate, which is very important for broadband response of the circulator. The inductance L at the central junction is a function of ω, M_s, and H, which translates to $L = L(\omega, M_s, \mu, \kappa)$. C_i is formed between each short stub and the metal ground, connected by inductance L_i. When applying a uniform static magnetic field along z direction, the permeability tensor is given by

$$[\mu_m] = \begin{bmatrix} \mu & jk & 0 \\ -jk & \mu & 0 \\ 0 & 0 & \mu_0 \end{bmatrix}, \tag{1}$$

where $\mu_{eff} = \mu\left[1-(\kappa/\mu)^2\right]$ the diagonal term μ and off-diagonal term k are functions of frequency ω, magnetic field H, and saturation magnetization M_s.

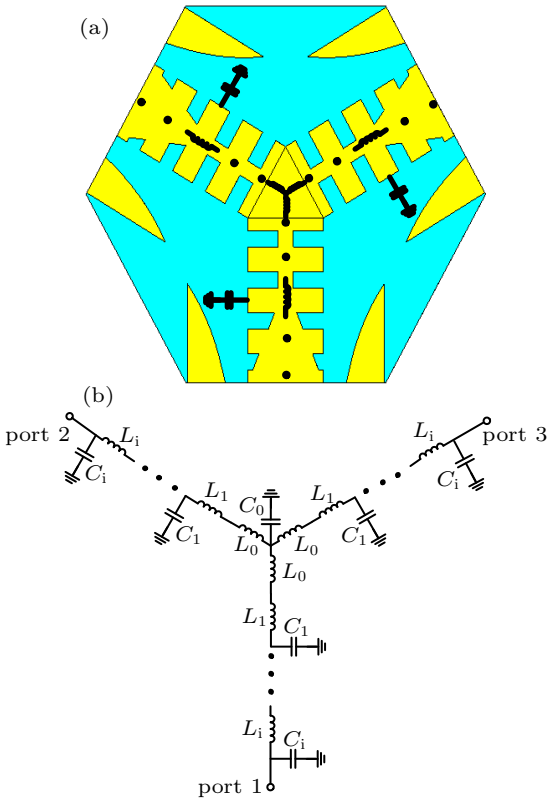


Fig. 3. Equivalent circuit model of the proposed plasmonic circulator.

According to the impedance matrix theory of three ports nonreciprocal network, the eigenvalues of the impedance matrix are determined as a function of frequency and circuit parameters.[38,40] The non-reciprocal junction impedance matrix Z can be used to find its three intrinsic impedances. According to three-port network series and parallel rules, eigenvalue algorithm can be used to find the eigenvalues corresponding to the impedance or admittance.[41] Using the relationship between the three-port scattering coefficients and impedances, S_{11}, S_{21}, and S_{31} are expressed as follows:

$$S_{11} = \frac{1}{3}(z_0 + z_+ + z_-), \tag{2a}$$

$$S_{21} = \frac{1}{3}(z_0 + z_+ e^{-i2\pi/3} + z_- e^{i2\pi/3}), \tag{2b}$$

$$S_{31} = \frac{1}{3}(z_0 + z_+ e^{i2\pi/3} + z_- e^{-i2\pi/3}), \tag{2c}$$

where z is the eigenvalue of the same-direction excitation, z_+ the eigenvalue of positive-phase excitation, and z the eigenvalue of negative-phase excitation.

The circuit model has been implemented in an advanced design software tool and the circuit model calculations have been matched with the simulation results. The S-parameter curves obtained by the equivalent circuit model are shown in Fig. 2(a) (blue curves). The results show that in the frequency

range of 6.0 GHz–9.0 GHz, the return loss and isolation are more than 11 dB while the minimum values are 50 dB and 35 dB, respectively. The *S*-parameters obtained from the simulations have been compared with the equivalent circuit model. It is clear from Fig. 2(a) that they show a very good agreement.

3. Fabrication and measurement

To verify the proposed design, we fabricated a plasmonic circulator prototype. The prototype is shown in Fig. 4, where figures 4(a)–4(e) represent SSPPs waveguide, metal ground plane, foam, ferrite, and permanent magnet, respectively. SSPPs waveguides have been fabricated using PCB technology. The permanent magnet is used to provide $H_0 = 1750$ Oe external magnetic field bias required for magnetizing ferrite. The material used for the ferrite disc is YX184 (MianYang Wei Qi Electronics Technology Co., Ltd.), which has a saturation magnetization of $4\pi M_s = 1850$ Gs, relative permittivity of $\varepsilon_f = 15$, and ferromagnetic resonance line width of $\Delta H = 10$ Oe. The foam sheet has been used to support and fix the ferrite disks. The complete prototype of plasmonic circulator is shown in Fig. 4(f) with the magnets placed symmetrically at the bottom and top of its ground plane. The Agilent Vector Network Analyzer (E5063A) has been used to measure *S*-parameters of the fabricated plasmonic circulator. The plasmonic circulator has been connected to the vector network analyzer through external coaxial cables and SMA connectors. Two ports of the plasmonic circulator have been connected to the input port and output port of the vector network analyzer while the third port has been connected to a matched 50-Ω load.

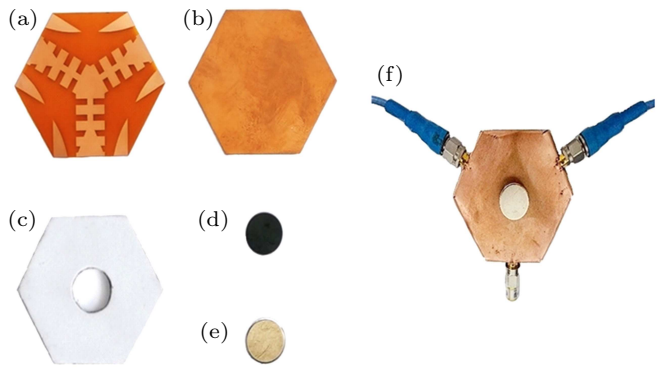


Fig. 4. Prototype of the fabricated plasmonic circulator. (a) SSPPs waveguide, (b) metal ground plane, (c) foam, (d) ferrite, (e) permanent magnet, and (f) overall structure.

The measured *S*-parameters have been shown in Fig. 5 (black curves). In the frequency range of 6.0 GHz–9.0 GHz, the isolation and return loss are more than 12 dB, and the insertion loss is better than 0.6 dB which is consistent with the simulation results as well. In comparison with the simulations, measured return loss is slightly lower and the measured insertion loss is slightly higher in the frequency range of 9.0 GHz–10.0 GHz. The difference between the simulation and experimental data may be explained through fabrication imperfections of plasmonic circulator. Consistency of simulated and measured data validates the simulation model. While the key performance parameters of the circulator confirms circulation of SSPPs.

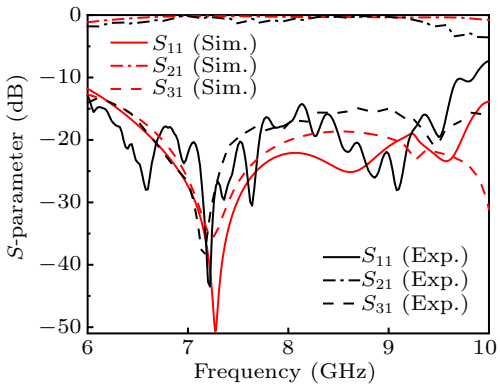


Fig. 5. Comparision of *S*-parameter of plasmonic circulator obtained from the simulation (Sim.) and the measurement (Exp.).

4. Conclusions

In conclusion, we have proposed a three-port, and rotationally symmetric plasmonic circulator based on non-reciprocal mode coupling. The modes inside the circular are SSPPs, which can propagate along the ultra-thin metallic comb plasmonic waveguides. The non-reciprocal mode coupling is enabled by the ferrite which is a gyromagnetic material having a permeability tensor with both diagonal and off-diagonal terms. By meeting impedance matching condition, the proposed circulator can operate in a broad frequency band of 6.0 GHz–10.0 GHz with insertion loss less than 0.5 dB. Furthermore, an equivalent circuit model has been employed to get a quantitative understanding. The circulator has been also validated by building a prototype and the results from simulations, circuit model, and measurements show a good agreement.

References

[1] Hines M E 1971 *IEEE Trans. Micro. Theory Tech.* **19** 442
[2] Qiu W, Wang Z and Marin S 2011 *Opt. Express* **19** 22248
[3] Dmitriev V, Kawakatsu M N and De Souza F J M 2012 *Opt. Lett.* **37** 3192
[4] Liu A Q, Khoo E H, Cheng T H, Li E P and Li J 2008 *Appl. Phys. Lett.* **92** 021119
[5] Shams S I, Elsaadany M and Kishk A A 2019 *IEEE Trans. Micro. Theory Tech.* **67** 94
[6] Bosma H 1964 *IEEE Trans. Microwave Theory Tech.* **12** 61
[7] Fay C E and Comstock R L 1965 *IEEE Trans. Microw. Theory Tech.* **MTT-13** 15
[8] Button K and Lax B 1956 *IEEE Trans. Anten. Propag.* **4** 531
[9] Afshani A and Wu K 2019 *IEEE Trans. Microw. Theory Tech.* **67** 3350

[10] Helszajn J 1984 *IEEE Trans. Microw. Theory Tech.* **MTT-32** 908

[11] Turki H, Huitema L, Monediere T, Lenoir B and Breuil C 2019 *IEEE Trans. Microw. Theory Tech.* **67** 845

[12] Liu K, Torki A and He S 2016 *Opt. Lett.* **41** 800

[13] Dmitriev V, Silva S and Castro W 2019 *Opt. Express* **27** 15982

[14] Yu Z, Veronis G, Wang Z and Fan S 2008 *Phys. Rev. Lett.* **100** 023902

[15] Jiang M, Zhu L and Zhu Q 2019 *Appl. Phys. Lett.* **114** 012408

[16] Hu B, Wang Q J and Zhang Y 2012 *Opt. Lett.* **37** 1895

[17] Li H P, Xia H D, Wang Z G, Zhang X X, Chen Y F, Zhang S J, Tang X G and Liu Y 2014 *Chin. Phys. B* **23** 024209

[18] Abdo B, Bronn N T, Jinka O, Olivadese S, Corcoles A D, Adiga V P, Brink M, Lake R E, Wu X, Pappas D P and Chow J M 2019 *Nat. Commun.* **10** 3154

[19] Shalaby M, Peccianti M, Ozturk Y and Morandotti R 2013 *Nat. Commun.* **4** 1558

[20] Shen Z, Zhang Y L, Chen Y, Sun F W, Zou X B, Guo G C, Zou C L and Dong C H 2018 *Nat. Comun.* **9** 1797

[21] Estep N A, Sounas D L, Soric J and Alù A 2014 *Nat. Phys.* **10** 923

[22] Pendry J B, Martín-Moreno L and Garcia-Vidal F J 2004 *Science* **305** 847

[23] Fang Y R and Sun M T 2015 *Light Sci. Appl.* **4** e294

[24] Chen L Y, Zong Z X, Gao J L, Tang S L and Du Y W 2019 *Chin. Phys. B* **28** 083302

[25] Shen X P, Cui T J, Martin-Cano D and Garcia-Vidal F J 2013 *Proc. Natl. Acad. Sci. USA* **110** 40

[26] Ma H F, Shen X P, Cheng Q, Jiang W X and Cui T J 2014 *Laser Photonics. Rev.* **8** 146

[27] Wang J. F, Qu S B, Ma H, Xu Z, Zhang A X, Zhou H, Chen H Y and Li Y F 2012 *Appl. Phys. Lett.* **101** 201104

[28] Shen X P and Cui T J 2013 *Appl. Phys. Lett.* **102** 211909

[29] Liu X, Feng Y, Chen K, Zhu B and Jiang T 2014 *Opt. Express* **22** 20107

[30] Gao X, Zhou L, Yu X Y, Cao W P, Li H O, Ma H F and Cui T J 2015 *Opt. Express* **23** 23270

[31] Liu X Y, Zhu L and Feng Y J 2016 *Chin. Phys. B* **25** 034101

[32] Wang J, Zhao L, Hao Z C and Cui T J 2018 *Appl. Phys. Lett.* **113** 071101

[33] Zhang H C, Zhang L P, He P H, Xu J and Cui T J 2020 *Light Sci. Appl.* **9** 113

[34] Pan J W, Wang J F, Qiu T S, Pang Y Q, Li Y F, Zhang J Q and Qu S B 2018 *AIP Adv.* **8** 055002

[35] Davies J B and Cohen P 1963 *IEEE Trans. Micro. Theory Tech.* **11** 506

[36] Konishi Y 1965 *IEEE Trans. Micro. Theory Tech.* **13** 852

[37] Zhao L, Zhang X, Wang J, Yu W, Li J, Su H and Shen X P 2016 *Sci. Rep.* **6** 36069

[38] Kianinejad A, Chen Z N and Qiu C W 2015 *IEEE Trans. Micro. Theory Tech.* **63** 1817

[39] Yu W, Luo G Q, Yu Y, Pan Y, Cao W, Pan Y and Shen Z 2019 *IEEE Trans. Anten. Propag.* **67** 1318

[40] Knerr R H, Barnes C E and Bosch A F 1971 *IEEE Trans. Micro. Theory Tech.* **18** 1100

[41] Konishi Y 1975 *IEEE Trans. Magn.* **11** 1262